


ORIGINAL ARTICLE

Open Access



Optimal delay for triple-phase hepatic computed tomography using a bolus-tracking technique in cats

Bin Li¹, Mingli Ren¹, Mahmoud M. Abouelfetouh^{1,2}, Panpan Guo¹, Ming Xing Ding¹, Diqi Yang¹, Yanqing Wu¹ and Yi Ding^{1*} 

Abstract

The objective of this study was to provide the characteristics of hepatic computed tomography images and optimize their transition delay with a bolus-tracking technique for triple-phase hepatic computed tomography in cats. Dynamic triple-phase computed tomography was performed in nine healthy cats. The upper third of the liver was dynamically scanned every 0.5 s for 40 s. The time density curves of the aorta and hepatic parenchyma mean enhancement were analyzed. Triple-phase hepatic computed tomography was performed three times with a bolus trigger of 200 Hounsfield units of aortic enhancement. The transition delays of the arterial, portal, and hepatic parenchymal phases were respectively 0, 5 and 60 s in the first scan; 2, 7 and 62 s in the second scan; and 4, 9 and 64 s in the third scan. All computed tomography images were evaluated by a certificated radiologist. The arterial vessels and their main branches were well enhanced at a 2 s transition delay. The contrast of the portal vein to the liver parenchyma was most obvious at a 7 s transition delay. The mean enhancement of the hepatic parenchyma peaked at a 62 s transition delay, whereas the degree of enhancement of the hepatic vasculature decreased. In this study, the recommended transition delays for the arterial, portal, and hepatic parenchymal phases were 2 s, 7 s and 62 s, respectively, after triggering at 200 Hounsfield units of aortic enhancement. This information may be helpful in diagnosing feline liver diseases and provides a key reference for the clinical implementation of CT.

Keywords: Bolus-tracking, CT, Feline, Liver, Triple-phase

Introduction

Liver function is dependent on adequate blood perfusion of the parenchyma. Outflow disturbances of the hepatic blood, including portosystemic shunts, portal hypertension and portal vein thrombosis are frequently observed in dogs and can also occur in cats (Van den Ingh et al. 1995; Lamb et al. 1996; Rogers et al. 2008; Respass et al. 2012). Computed tomography angiography (CTA), with its high spatial and contrast resolution, is helpful to intuitively visualize portal vein obstructions or shunts. In

dogs and humans, triple-phase helical computed tomography (CT) has been proposed as a valuable technique for detecting hepatic vascular or parenchymal abnormalities (Vauthey et al. 1997; Zwingerberger et al. 2005; Stieger et al. 2007). It has been reported that CTA is more reliable for detecting portal vein thrombosis than ultrasound in dogs (Von Stade 2021).

Triple-phase hepatic CT consists of the arterial, portal, and hepatic parenchymal phases, which are evaluated according to the attenuation changes in the liver and associated vasculature after a contrast agent is intravenously injected. The arterial and portal phases can provide accurate information regarding the hemodynamic changes in the hepatic artery and portal vein, whereas liver

* Correspondence: dingyi@hzau.edu.cn

¹College of Veterinary Medicine, Huazhong Agricultural University, Wuhan, Hubei Province 430070, P. R. China

Full list of author information is available at the end of the article



© The Author(s). 2022 **Open Access** This article is licensed under a Creative Commons Attribution 4.0 International License, which permits use, sharing, adaptation, distribution and reproduction in any medium or format, as long as you give appropriate credit to the original author(s) and the source, provide a link to the Creative Commons licence, and indicate if changes were made. The images or other third party material in this article are included in the article's Creative Commons licence, unless indicated otherwise in a credit line to the material. If material is not included in the article's Creative Commons licence and your intended use is not permitted by statutory regulation or exceeds the permitted use, you will need to obtain permission directly from the copyright holder. To view a copy of this licence, visit <http://creativecommons.org/licenses/by/4.0/>. The Creative Commons Public Domain Dedication waiver (<http://creativecommons.org/publicdomain/zero/1.0/>) applies to the data made available in this article, unless otherwise stated in a credit line to the data.

parenchymal lesions such as inflammation, neoplasia, or masses can be detected in the hepatic parenchymal phase (Leela-Arporn 2019). Whether in humans or animals, the quality of enhanced CT can be ultimately influenced by several external factors: (1) patient-related, such as body weight and cardiac function; (2) contrast agent-related, such as the iodine content, infusion duration and rate, and the size of a catheter by which it is infused into the cephalic vein; and (3) scanning-related, such as the method and delay time of scanning (Heiken et al. 1995; Berland and Lee 1988; Bae 2010; Makara et al. 2015; Lee et al. 2017; Thierry et al. 2018).

An appropriate scan delay is needed for contrast-enhanced CT to acquire adequate enhancement of the arterial, portal, and hepatic parenchymal phases, which is critical for generating two-dimensional (2-D) and three-dimensional (3-D) angiographic images (Berland and Lee 1988). However, there is a lack of relevant research, and the scan delay time used in humans is not suitable for dogs and cats. A bolus-tracking technique can optimize the delay time for each hepatic phase, irrespective of individual cardiovascular dynamics. After the region of interest (ROI) threshold is reached, the scanner will have a preprogrammed transition delay (TD) before initiating the CTA scan to acquire optimal visualization of the bolus (Saade et al. 2011). The TD, defined as the delay between the time at which the ROI threshold is reached and the time when the actual CTA scan starts, is a pivotal parameter of the bolus-tracking technique to obtain a high-quality CTA. Optimal scan delays for multiphase CT using the bolus-tracking technique in the canine pancreas (Soo-Young et al. 2015) and kidneys (Cho et al. 2018) have been reported.

Triple-phase CTA separates the arterial phase from the portal and systemic venous phases to allow a comprehensive assessment of vascular abnormalities or parenchymal lesions. CTA has been used to prompt the diagnosis of extrahepatic arteriportal fistulae (Choi et al. 2018) and to confirm the absence of the portal vein (Holloway et al. 2018) in cats. The size, attenuation and enhancement pattern of the pancreas (Secrest et al. 2017), biliary tract (Pilton et al. 2019) and vascular anatomy of the kidneys (Damri and Nan 2019) using multiphase CTA in healthy cats have also been described. However, there is a paucity of information regarding triple-phase hepatic CT, and no study has described the optimal TDs for triple-phase hepatic helical CT using a bolus-tracking technique in cats. Therefore, the aims of this study were to describe the multiphase CT characteristics and to explore the optimal TDs for triple-phase hepatic helical CT using a bolus-tracking technique in healthy cats.

Results

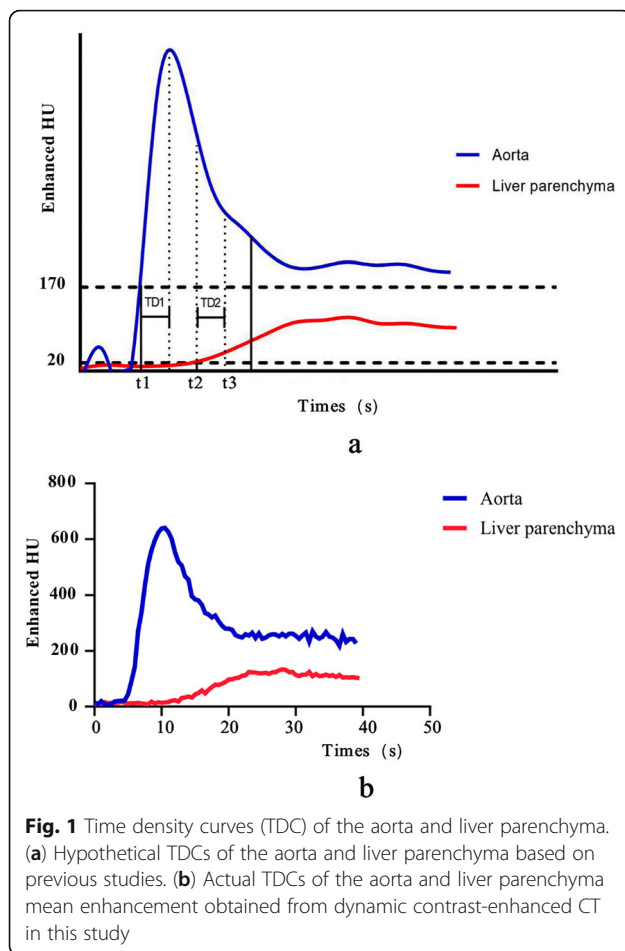
Time setting for exploring the TDs of the arterial, portal and delay phases

To facilitate the analysis, time density curves (TDCs) of the aorta and liver parenchyma were assessed based on the current studies, and t1, t2 and t3 were three proposed time points on the time axis (Fig. 1). In Fig. 1a, t1 was presumed to represent the time at which the aorta CT value reached a threshold of 200 HU, whereas t2 and t3 were assigned to the time points for the termination of the arterial and portal phases, respectively. TD1 and TD2 represent the periods of the arterial and portal phases, respectively. Given the scanning time of the entire liver (2.7 s) and the CT table movement (1 s), high-quality three-phase hepatic CT images could be acquired if TD1 and TD2 met the following conditions: $(1 + 2.7) \leq (1 + 2.7 + \text{TD1}) \leq (t2 - t1)$ and $t2 - (\text{TD1} + 2.7 + 1) \leq (\text{TD2} + 2.7 + 1) \leq (t3 - t2)$. The actual TDCs of aorta and liver parenchymal enhancement are shown in Fig. 1b, where the measured values of t1, t2, and t3 were 6.11 ± 1.08 s, 10.94 ± 1.57 s, and 24 ± 3.32 s, respectively. The final conditions were set as $0 \leq \text{TD1} \leq 1.13 \pm 1.09$ s and $0 \leq \text{TD2} \leq 9.33 \pm 3$ s. Therefore, 0 s, 2 s and 4 s were selected to explore the optimal TD of the arterial phases. Similarly, 5 s, 7 s and 9 s were assigned to explore the portal phase. For the hepatic parenchymal phase, a longer time is required for the contrast agent to be removed from the hepatic veins and liver parenchyma. Therefore, we chose 60 s, 62 s and 64 s to explore the TDs of delay phase for the hepatic parenchyma.

CT values and triple-phase CT images of feline liver

CT values of the aorta and hepatic parenchyma were measured by placing the ROI at the center of these organs, respectively. The mean CT values of them on the precontrast CT were 28.00 ± 2.88 HU and 53.63 ± 3.20 HU, respectively. The enhancements of these two organs in the arterial, portal, and hepatic parenchymal phases are shown in Table 1.

CT images were transferred to a workstation using 3-D reconstruction to obtain volume rendering (VR) and MIP images. Triple-phase hepatic CT 3-D reconstruction images of the arterial, portal, and hepatic parenchymal phases are shown in Figs. 2, 3 and 4, respectively. In the arterial phase, the aorta was enhanced, but the hepatic arteries did not become contrast-enhanced with a 0 s TD. The arterial vessels and their main branches were clearly seen with a 2 s TD, whereas the portal vein lumens were slightly enhanced at a 4 s TD (Fig. 2a, b and c). The VR images of the arterial phase at a 0 s TD displayed the arterial trunk and hepatic arterial trunk. The hepatic arterial branches as well as the portal vein were



visible at a 2 s TD. The enhancement of the arterial blood vessels was inconspicuous in the VR images at a 4 s TD (Fig. 2d, e and f). Furthermore, at a 2 s TD, the arterial branches and portal veins were significantly enhanced on the MIP (Fig. 2g, h and i). In the portal venous phase (Fig. 3), the enhancement of the posterior vena cava was not evident at a 5 s TD. The portal vein branches were notably visualized at a 7 s TD. The posterior vena cava and hepatic veins did not become hyperattenuating at a 9 s TD. These vascular characterizations observed in the CT images were similar to those in the VR and MIP images. In the hepatic parenchymal phase (Fig. 4), there was substantial contrast residue in

the blood vessels, hepatic artery, and portal vein, and hepatic vein were still apparent at a 60 s TD. However, the aorta, hepatic arteries, portal veins and outlines were blurred at a 64 s TD.

Characteristics of hepatic vascular anatomy on triple-phase hepatic CT images

Triple-phase hepatic CT images are shown in Fig. 5. In the arterial phase (Fig. 5a), hepatic arteries (red arrow) and partly enhanced portal vein lumens were observed. In the portal venous phase (Fig. 5b), portal vein (red triangles) branches were hyperenhanced, whereas in the portal phase (Fig. 5c), the contrast agents were transferred to the hepatic veins (red triangle). The VR images of the hepatic vascular anatomy at three delay times are shown in Fig. 6. In the arterial phase (Fig. 6a), the arteries can be clearly observed, and the anterior mesenteric artery and the celiac artery can also be easily distinguished separate from the aorta. The celiac artery divided into the splenic artery, the left gastric artery, and the hepatic artery. The hepatic artery divided into left and right branches. In the portal phase (Fig. 6b), the main portal vein can be clearly seen. The main portal vein divided into the left branch and the right branch at the hepatic portal as well as many sub-branches. In the hepatic parenchymal phase (Fig. 6c), the hepatic vein and portal vein are clearly seen, and the branches of the hepatic vein can also be clearly observed. The blood vessels of the hepatic vein and portal vein are well developed and intertwined. The main hepatic vein joins the posterior vena cava at the second hepatic portal.

Discussion

In this study, triple-phase CT for scanning feline livers in conjunction with a bolus-tracking technique was performed successfully in all cats. The CT values of the hepatic parenchyma in our study on precontrast CT (53.80 ± 6.42 HU) were similar to those reported in dogs (51.2–65.5 HU) (Lee et al. 2017). The aortic CT value was 28.00 ± 2.50 HU, which differs from those reported in dogs (36.6–51.0 HU) (Lee et al. 2017). The discrepancy in CT attenuation of the aorta between the normal dogs and cats may be due to ROI placement and/or species differences. In addition, the CT value is related to

Table 1 Mean enhancements (HU) of the aorta and hepatic parenchyma in the arterial, portal and hepatic parenchymal phases

ROI	Arterial phase				Portal phase		Hepatic parenchymal phase		
	0 s	2 s	4 s	5 s	7 s	9 s	60 s	62 s	64 s
Aorta	394.8 ± 26.57^a	479.2 ± 47.43^b	560.7 ± 43.35^c	588.7 ± 18.96^a	466.1 ± 15.98^b	342.0 ± 29.91^c	164.4 ± 19.39^a	207.1 ± 12.55^b	107.3 ± 9.05^c
Hepatic parenchyma	13.46 ± 1.14^a	19.54 ± 4.57^b	26.90 ± 5.63^c	46.78 ± 1.62^a	58.10 ± 12.09^a	97.29 ± 16.20^b	68.23 ± 16.15^a	81.22 ± 10.61^a	49.03 ± 12.86^b

The values are shown as the mean \pm standard deviation. HU Hounsfield Units, ROI region of interest. Values with different letters among the three transition delay time points of the arterial, portal or hepatic parenchymal phase differ significantly ($P < 0.05$) based on a one-way ANOVA with the least significant difference method

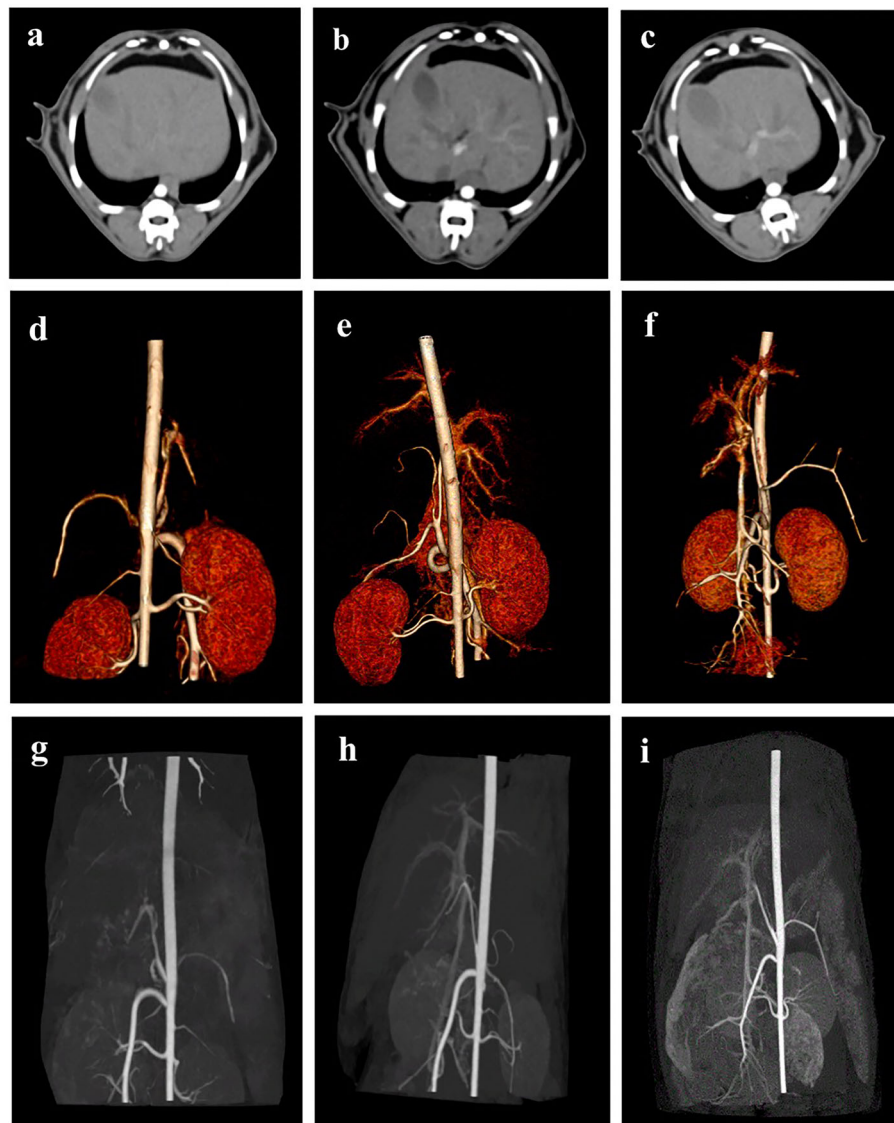


Fig. 2 Triple-phase hepatic CT images of the arterial phase at different TDs (0 s, 2 s and 4 s). The arterial phase images at 0 s TD: hepatic transverse CT image (a), hepatic vessels VR image (d) and MIP image (g). The arterial phase images at 2 s TD: hepatic transverse CT image (b), hepatic vessel VR image (e) and MIP image (h). The arterial phase images at 4 s TD: hepatic transverse CT image (c), hepatic vessel VR image (f) and MIP image (i). All images have the same orientation; R is on the left of the images

the scan parameters, the dose and infusion rate of contrast agents, and catheter size (Cademartiri et al. 2002; Kayan et al. 2016; Lee et al. 2017).

TDC of the aortic enhancement derived from dynamic contrast-enhanced CT presents as a downward parabola; there was a sharp and rapid peak enhancement (approximately 660 HU) with a subsequent rapid drop in attenuation. The TDC of hepatic parenchyma enhancement differed greatly from that of the aorta, gradually increasing to approximately 160 HU and then declining steadily. The shapes of the aortic and hepatic parenchyma TDCs in this research were similar to those reported

previously (Ichikawa et al. 2006). TDCs of the aorta and liver parenchyma provided a reference for the delay time of the bolus-tracking technique used in triple-phase hepatic CT, which avoided repeated exploration of the scan parameters and excessive exposure of the animals to radiation and contrast agents.

For the scanning protocol used in triple-phase hepatic CT, the hepatic artery and its branches were all completely displayed at a 2 s TD compared with a 0 s TD or a 4 s TD. Although the hepatic artery mean enhancement peaked at a 4 s TD, it did not differ significantly from that at the 2 s TD. Thus, a 2 s TD after the bolus

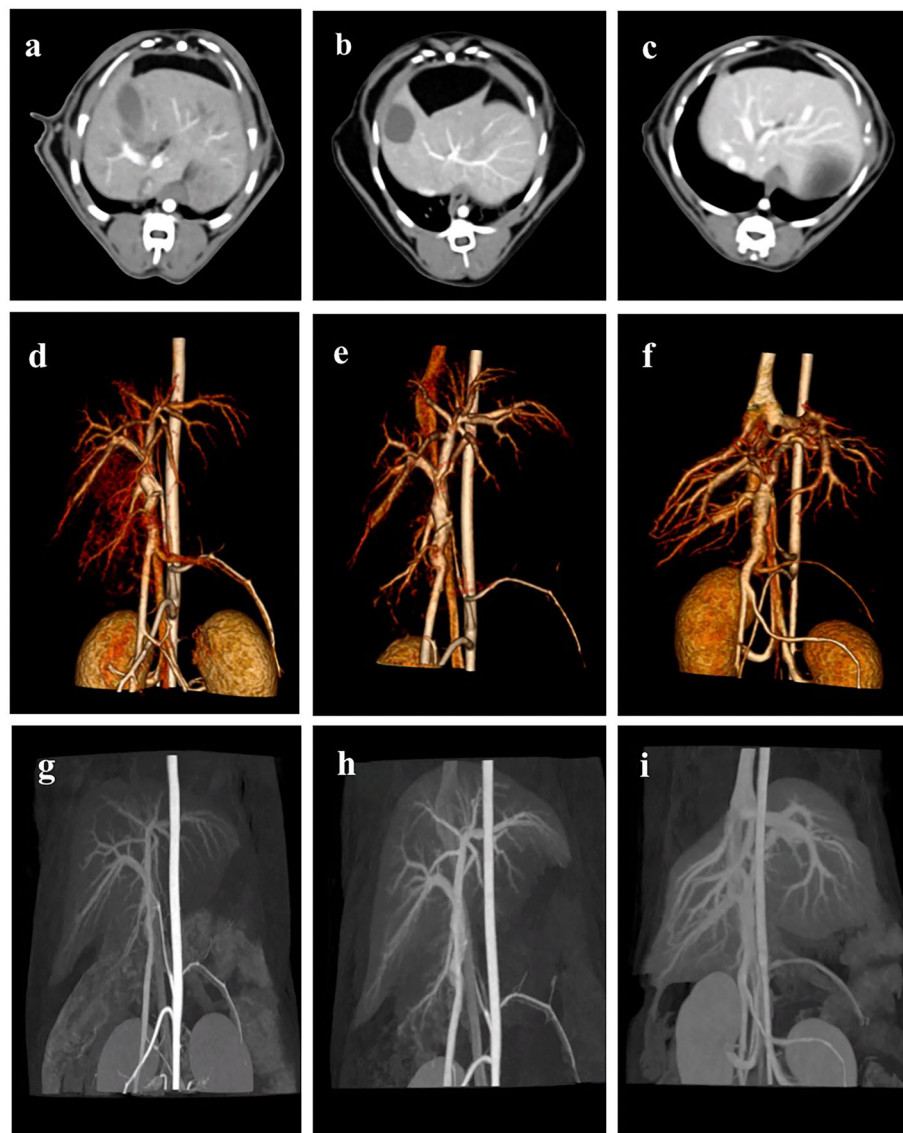


Fig. 3 Triple-phase hepatic CT images of the portal phase at different TDs (5 s, 7 s and 9 s). Portal venous phase images at 5 s TD: hepatic transverse CT image (a), hepatic vessel VR image (d) and MIP image (g). The portal venous phase images at 7 s TD: hepatic transverse CT image (b), hepatic vessels VR image (e) and MIP image (h). The portal venous phase images at 9 s TD: hepatic transverse CT image (c), hepatic vessels VR image (f) and MIP image (i). All images have the same orientation; R is on the left of the images

trigger is optimal for visualizing the hepatic artery in this study. In the portal phase, the main branch of the portal vein, rather than the posterior vena cava, was clearly seen on the triple phase CT images at a 7 s TD compared with those at a 5 s TD and a 9 s TD. Therefore, 7 s was the optimal TD for the portal phase. The scan delay of the portal phase in our study was shorter than that reported in humans (13~15 s) (Nakai et al. 2011) and dogs (12 s) (Zwingenberger et al. 2005). This difference is due to a larger volume of contrast agent injected in humans and dogs, which can shift the time/attenuation curve upward and to the right (Cademartiri et al. 2002). Thus, when the

contrast agent volume is large, the time to the maximum enhancement peak is increased. This study showed that the degree of enhancement of the hepatic vasculature decreased, whereas the mean enhancement of the liver parenchyma peaked at a 62 s TD. Therefore, 62 s was determined to be the TD representative of the hepatic parenchymal phase, which contributes to the detection of liver parenchymal lesions such as inflammation and neoplasia based on dog and human references (Soyer et al. 2004; Taniura et al. 2009; Leela-Arporn et al. 2019).

An appropriate scan delay is essential to acquire high-quality CTA. To date, the scan delay has been

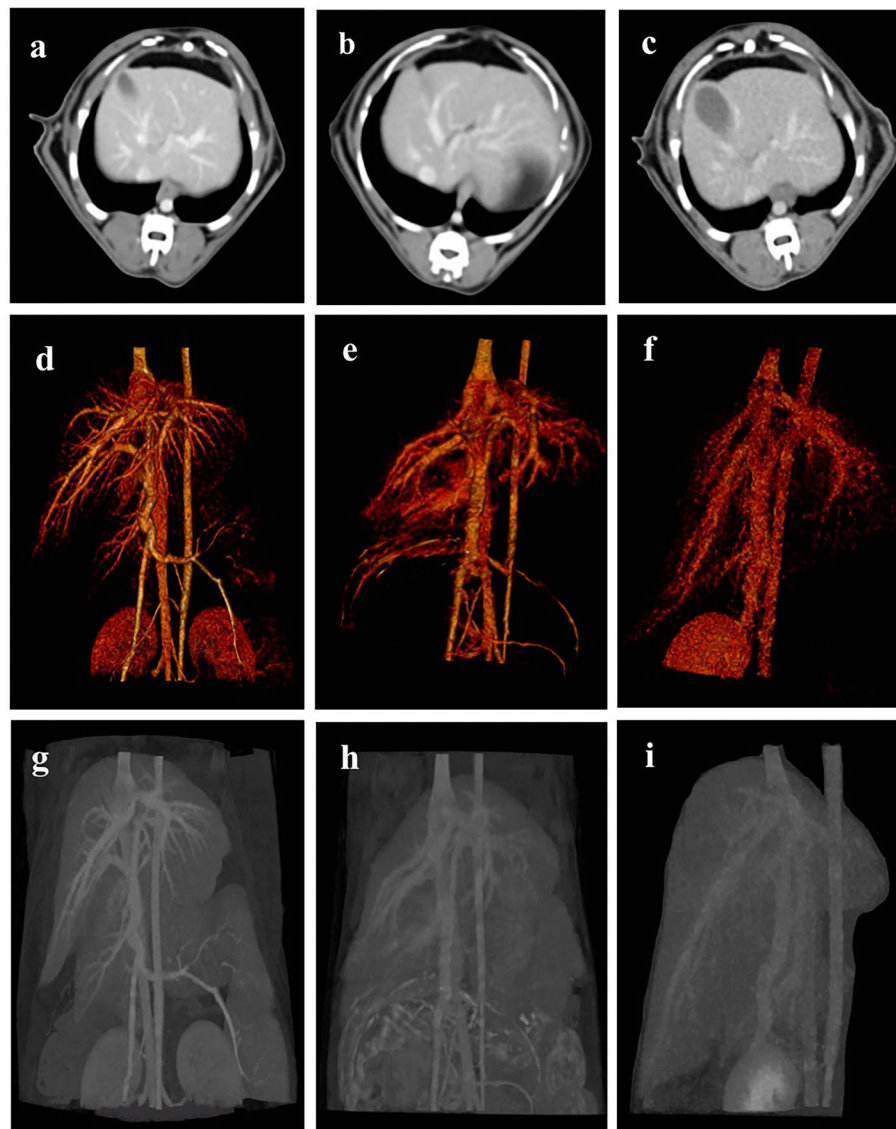


Fig. 4 Triple-phase hepatic CT images of the delay phase at different TDs (60 s, 62 s and 64 s). Hepatic parenchymal phase images at 60 s TD: hepatic transverse CT image (**a**), hepatic vessel VR image (**d**) and MIP image (**g**). Hepatic parenchymal phase images at 62 s TD: hepatic transverse CT image (**b**), hepatic vessel VR image (**e**) and MIP image (**h**). Hepatic parenchymal phase images at 64 s TD: hepatic transverse CT image (**c**), hepatic vessel VR image (**f**) and MIP image (**i**). All images have the same orientation; R is on the left of the images

investigated using fixed scan delay, test-bolus and bolus-tracking techniques. The fixed scan delay is estimated based on experience in CTA, typically ranging from 10 s to 35 s, which is easy to perform but may miss peak enhancement of the tissues (Saade et al. 2011). In the test-bolus technique, a small amount of a contrast agent is infused at the same rate as the main bolus, and a single-level low-dose dynamic scan is performed at determined time intervals. The time between the start of the test bolus injection and a determined point of the time/attenuation curve of the test bolus is used as the delay time for the injection of the main bolus (Cademartiri

et al. 2002). In the bolus-tracking technique, a trigger attenuation value (threshold) is arbitrarily chosen before starting the CTA data acquisition. A single-level low-dose dynamic scan is performed at determined time intervals during the injection of a contrast agent. A CT scan is started after reaching the triggering threshold (Cademartiri et al. 2002). Bolus tracking provides better timing of CT scans in relation to the time/attenuation curve and avoids the need for additional contrast agent administration (Stieger et al. 2007). Therefore, in this study, a bolus-tracking technique was used to explore the triple-phase CT of the feline liver, and the ROI was

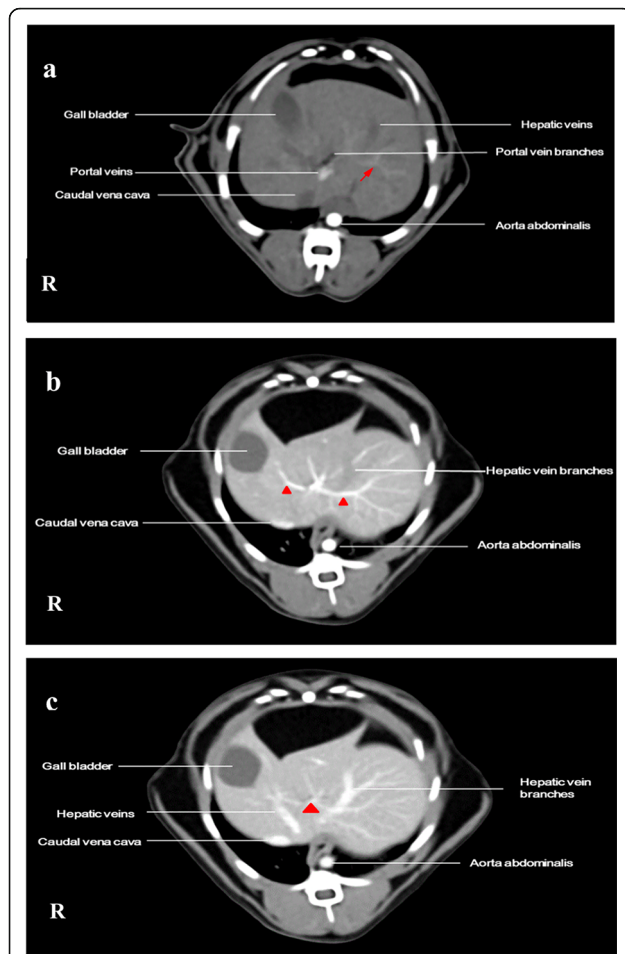


Fig. 5 CT images of hepatic vascular anatomy at three different delay times in cats. Hepatic arteries (red arrow) and partly enhanced portal vein lumens were seen in the arterial phase (a). In the portal venous phase (b), portal vein (red triangles) branches were hyperenhanced, whereas in the portal phase (c), the contrast agents were transferred to hepatic veins (red triangle). CT images were analyzed in a soft tissue window (W/L: 400/40)

placed inside the vessel lumen of the aorta, which was easily identified on precontrast CT.

In the arterial phase at a 2 s TD, the hepatic artery branches were enhanced incompletely, possibly because 1) feline hepatic arteries are narrow; 2) the subsegmental branches of the hepatic artery were not completely perfused by the contrast agent; and 3) the distal hepatic arteries were automatically removed during image reconstruction based on having a density similar to that of the hepatic parenchyma. Moreover, portal vein enhancement occurred during the arterial phase. This may result from rapid blood flow from the anterior mesenteric, posterior mesenteric, and splenic arteries transporting the contrast agent to the portal vein, resulting in a slight overlap between the hepatic artery and portal vein. The TD data from our study provide a useful reference for diagnosing

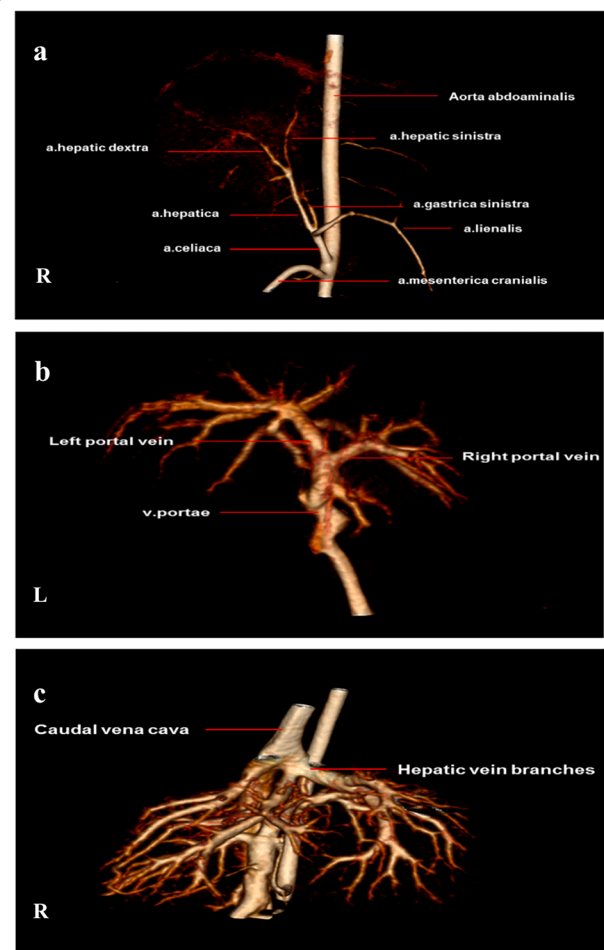


Fig. 6 VR images of hepatic vascular anatomy at different delay times in cats. (a) The arterial phase, (b) the portal phase and (c) the hepatic parenchymal phase

hepatic blood outflow disturbances or parenchymal lesions. However, their reliability under pathological states still needs to be further verified.

Conclusions

In conclusion, this research established the characteristics and optimized scan delays of triple-phase hepatic CT in cats. The optimal TDs recommended in our scan protocol for arterial, portal, and hepatic parenchymal phases in triple-phase CT were 2, 7, and 62 s, respectively, after triggering at 200 HU of aortic enhancement using a bolus-tracking technique; this provides a basis for diagnosing and evaluating feline hepatic blood outflow related to liver disease or parenchymal lesions.

Methods

Animals

This study was approved by the College of Veterinary Medicine, Huazhong Agricultural University, Wuhan,

China (HZAUCA-2019-008). Nine adult domestic cats (4 males and 5 females, 2~3 years, 3.5~4.5 kg body weight) without any history or clinical signs of systemic illness were dewormed and housed together in a comfortable environment. The cats were considered healthy based on the recorded history and the findings of physical examination, serum biochemistry, electrocardiogram, and abdominal ultrasonography. For all included cats, general anesthesia was administered with an intravenous injection of 5~7.5 mg/kg Zoletil (Virbac, Carros, France). CT scanning was started when the animals were in the second stage of surgical anesthesia.

Computed tomography protocol

All hepatic CT scans were performed on a 64-row multi-detector CT (Aquilion Prime 128, Canon, Japan). Prior to the dynamic scan, a survey scan of the entire abdomen was performed to identify the scan horizontal location of the liver. The upper third of the liver was then immediately scanned every 0.5 s until 40 s after the injection of a contrast agent (Omnipaque 350, 350 mgI/mL, GE Healthcare, Cork, Ireland). To obtain TDCs of the aorta and hepatic parenchyma enhancement, the contrast agent dose (1.5 mL/kg) was injected using a power injector (SinoPower-D, Sino Medical-Device, Shenzheng, China) at a rate of 0.5 mL/s through a 24 G catheter placed in the right cephalic vein. The main dynamic contrast-enhanced CT parameters were set as follows: 100 kV, 160 mA, 2 mm slice thickness, and 0.5 s rotation time.

Triple-phase hepatic CT was performed after bolus tracking was triggered at 200 Hounsfield units (HU) of aortic enhancement. Nine cats underwent the first triple-phase CT on Day 1 of the experiment; the TDs of the arterial, portal, and hepatic parenchymal phases were 0, 5, and 60 s, respectively. The second scan (TDs of 2, 7 and 62 s) and the third scan (TDs of 4, 9 and 64 s) were conducted on Days 8 and 16, respectively. The contrast agent and saline were intravenously injected at a dose of 1.5 mL/kg and a rate of 0.5 mL/s before each scan. The triple-phase hepatic CT parameters were set as follows: 150~180 kV, 160 mA, 5 mm slice thickness and 0.5 s rotation time. The images were reconstructed using 2 mm thickness and 2 mm intervals. The times for the entire liver and for table motion were 2.7 s and 1 s, respectively.

Image analysis

The CT images were transferred to a workstation (Radio Force, Japan). All CT images were evaluated with a soft tissue window (window width/window level: 400/40). The CT values of aorta and hepatic parenchyma attenuation were measured by placing the ROI (16 mm²) at the center of the aorta and hepatic parenchyma, respectively, on CT images, during the precontrast, arterial, portal, and hepatic parenchymal phases. The CT measurements

were repeated three times at each TD time point, and the mean values were represented as CT values (HU) of the aorta or hepatic parenchyma at the TD time point for each cat. All CT images were viewed and analyzed by a qualified professional veterinarian (with over 5 years of experience on CT) using VR and MIP (maximum intensity projection). The 3-D reconstruction was achieved via automatic bone removal and virtual cutting tools.

Data analysis

All data are expressed as the mean \pm standard deviation. Statistical analyses were performed using SPSS V. 18.0 (SPSS Inc., Chicago, IL, USA). CT values among the different TDs of the arterial, portal or hepatic parenchymal phase were compared using a one-way analysis of variance with the least significant difference method. Differences were considered significant if *P* values were less than 0.05.

Abbreviations

CTA: Computed tomography angiography; CT: Computed tomography; 2-D: Two-dimensional; 3-D: Three-dimensional; ROI: Region of interest; TD: Transition delay; TDC: Time density curve; HU: Hounsfield units; VR: Volume rendering; MIP: Maximum intensity projection

Acknowledgments

Not applicable.

Authors' contributions

All authors contributed to the conception and design of the study. BL, MLR, MMA, PPG, MXD, DQY, YQW, YD, performed the experiments. BL, MLR, MXD and YD analyzed the data. BL and MLR wrote the manuscript. All authors read and approved the final manuscript.

Funding

This study was supported by the National Natural Science Foundation of China (Nos: 31802255, 31972756 and 32072938). We would like to thank all participants who worked for this study.

Availability of data and materials

Not applicable.

Declarations

Ethics approval and consent to participate

The animal experiment in this study was approved by the College of Veterinary Medicine, Huazhong Agricultural University, Wuhan, China (HZAUCA-2019-008).

Consent for publication

Not applicable.

Competing interests

Authors Mingxing Ding and Yi Ding were not involved in the journal's review or decisions related to this manuscript.

Author details

¹College of Veterinary Medicine, Huazhong Agricultural University, Wuhan, Hubei Province 430070, P. R. China. ²College of Veterinary Medicine, Benha University, Moshtohor, Egypt.

Received: 16 December 2021 Accepted: 29 March 2022

Published online: 26 April 2022

References

- Bae, K.Y. 2010. Intravenous contrast medium administration and scan timing at CT: considerations and approaches. *Radiology* 256 (1): 32–61. <https://doi.org/10.1148/radiol.10090908>.
- Berland, L.L., and J.Y. Lee. 1988. Comparison of contrast media injection rates and volumes for hepatic dynamic incremented computed tomography. *Investigative Radiology* 23 (12): 918–922. <https://doi.org/10.1097/00004424-198812000-00008>.
- Cademartiri, F., A. Van der Lugt, G. Pavone Luccichenti, P. Krestin, and G. P. 2002. Parameters affecting bolus geometry in CTA: A review. *Journal of Computer Assisted Tomography* 26 (4): 598–607. <https://doi.org/10.1097/00004728-200207000-00022>.
- Cho, H., D.H. Lee, A.Y. Cha, D.E. Kim, D.W. Chang, and J. Choi. 2018. Optimization of scan delay for multi-phase computed tomography by using bolus tracking in normal canine kidney. *Journal of Veterinary Medical Science* 19 (2): 290–295. <https://doi.org/10.14142/jvs.2018.19.2.290>.
- Choi, M., H. Kim, J. Yoon, and M. Choi. 2018. CT features of extrahepatic arterioportal fistula in two cats. *Journal of Small Animal Practice* 60 (11): 697–700. <https://doi.org/10.1111/jsap.12957>.
- Damri, D., and C. Nan. 2019. Morphological assessment of cat kidneys using computed tomography. *Anatomia, Histologia, Embryologia* 48 (4): 358–365. <https://doi.org/10.1111/ahc.12448>.
- Heiken, J.P., J.A. Brink, B.L. McClennan, S.S. Sagel, T.M. Crowe, and M.V. Gaines. 1995. Dynamic incremental CT: Effect of volume and concentration of contrast material and patient weight on hepatic enhancement. *Radiology* 195 (2): 353–357. <https://doi.org/10.1148/radiology.195.2.7724752>.
- Holloway, A., L. Groot, and K. van der Schaaf. 2018. Congenital absence of the portal vein in a cat. *Journal of Feline Medicine and Surgery Open Reports* 4 (1): 2055116917749079. <https://doi.org/10.1177/2055116917749079>.
- Ichikawa, T., S.M. Erturk, and T. Araki. 2006. Multiphasic contrast-enhanced multidetector-row CT of liver: Contrast-enhancement theory and practical scan protocol with a combination of fixed injection duration and patients' body-weight-tailored dose of contrast material. *European Journal of Radiology* 58 (2): 165–176. <https://doi.org/10.1016/j.ejrad.2005.11.037>.
- Kayan, M., H. Demirtas, Y. Türkmen, F. Kayan, G. Getinkaya, M. Kara, A.O. Celik, A. Umul, O. Yilmaz, and A.R. Aktas. 2016. Carotid and cerebral CT angiography using low volume of iodinated contrast material and low tube voltage. *Diagnostic and Interventional Imaging* 97 (11): 1173–1179. <https://doi.org/10.1016/j.diii.2016.06.005>.
- Lamb, C.R., R.H. Wrigley, K.W. Simpson, M.F. Hifft, O.A. Garden, G.B. Smyth, C. Rutgers, and R.N. White. 1996. ULTRASONOGRAPHIC DIAGNOSIS OF PORTAL VEIN THROMBOSIS IN FOUR DOGS. *Veterinary Radiology & Ultrasound* 37 (2): 121–129. <https://doi.org/10.1111/j.1740-8261.1996.tb01209.x>.
- Lee, S.K., D. Lee, D. Kim, A. Cha, and J. Choi. 2017. Effect of catheter size and injection rate of contrast agent on enhancement and image quality for triple-phase helical computed tomography of the liver in small dogs. *Veterinary Radiology & Ultrasound* 58 (6): 664–670. <https://doi.org/10.1111/vru.12533>.
- Leela-Arpon, R., H. Ohta, G. Shimbo, G. Shimbo, K. Hanazono, T. Osuga, K. Morishita, N. Sasaki, and M. Takiguchi. 2019. Computed tomographic features for differentiating benign from malignant liver lesions in dogs. *Journal of Veterinary Medical Science* 81 (12): 1697–1704. <https://doi.org/10.1292/jvms.19-0278>.
- Makara, M., J. Chau, E. Hall, H. Kloeppel, J. Podadera, and V. Barrs. 2015. Effect of two contrast injection protocols on feline aortic and hepatic enhancement using dynamic computed tomography. *Veterinary Radiology & Ultrasound* 56 (4): 367–373. <https://doi.org/10.1111/vru.12239>.
- Nakai, M., M. Sato, A. Ikoma, K. Nakata, S. Sahara, I. Takasaka, H. Minamiguchi, N. Kawai, T. Sonomura, and K. Kishi. 2011. Triple-phase computed tomography during arterial portography with bolus tracking for hepatic tumors. *Japanese Journal of Radiology* 28 (2): 149–156. <https://doi.org/10.1007/s11604-009-0399-z>.
- Pilton, J.L., J. Chau, T.S. Foo, E.J. Hall, F. Martinez-Taboada, J.M. Podadera, and M.A. Makara. 2019. Hepatic computed tomography and cholangiography by use of gadoteric acid in healthy cats. *Journal of Veterinary Research* 80 (4): 385–395. <https://doi.org/10.2460/ajvr.80.4.385>.
- Respass, M., T.E. O'Toole, O. Taeymans, C.L. Roger, A. Johnston, and C.R.L. Webster. 2012. Portal vein thrombosis in 33 dogs: 1998–2011. *Journal of Veterinary Internal Medicine* 26 (2): 230–237. <https://doi.org/10.1111/j.1939-1676.2012.00893.x>.
- Rogers, C.L., T.E. O'Toole, J.H. Keating, D.G. Penninck, and C.R.L. Webster. 2008. Portal vein thrombosis in cats: 6 cases (2001–2006). *Journal of Veterinary Internal Medicine* 22 (2): 282–287. <https://doi.org/10.1111/j.1939-1676.2012.00893.x>.
- Saade, C., R. Bourne, M. Wilkinson, and P. Brennan. 2011. Contrast medium administration and parameters affecting bolus geometry in multidetector computed tomography angiography: An overview. *Journal of Medical Imaging and Radiation Oncology* 42 (3): 113–117. <https://doi.org/10.1016/j.jmir.2011.05.002>.
- Secrest, S., A. Sharma, and A. Bugbee. 2017. Triple phase computed tomography of the pancreas in healthy cats. *Veterinary Radiology & Ultrasound* 59 (2): 163–168. <https://doi.org/10.1111/vru.12577>.
- Soo-Young, C., C. Ho-Jung, L. Ki-Ja, and Y.W. Lee. 2015. Establishment of optimal scan delay for multi-phase computed tomography using bolus-tracking technique in canine pancreas. *Journal of Veterinary Medical Science* 77 (9): 1049–1054. <https://doi.org/10.1292/jvms.14-0693>.
- Soyer, P., M. Pocard, M. Boudiaf, M. Abitbol, L. Hamzi, Y. Panis, P. Valleur, and R. Rymer. 2004. Detection of hypovascular hepatic metastases at triple-phase helical CT: sensitivity of phases and comparison with surgical and histopathologic findings. *Radiology* 231 (2): 413–420. <https://doi.org/10.1148/radiol.2312021639>.
- Stieger, S.M., A. Zwingenberger, R.E. Pollard, A.E. Kyles, and E.R. Wisner. 2007. Hepatic volume estimation using quantitative computed tomography in dogs with portosystemic shunts. *Veterinary Radiology & Ultrasound* 48 (5): 409–413. <https://doi.org/10.1111/j.1740-8261.2007.00268.x>.
- Taniura, T., K. Marukawa, K. Yamada, Y. Hikasa, and K. Ito. 2009. Differential diagnosis of hepatic tumor-like lesions in dog by using dynamic CT scanning. *Journal of Veterinary Medical Science* 58 (1): 17–24. <https://doi.org/10.1490553>.
- Thierry, F., J. Chau, M. Makara, S. Specchi, E. Auriemma, M. Longo, I. Handel, and T. Schwarz. 2018. Vascular conspicuity differs among injection protocols and scanner types for canine multiphasic abdominal computed tomographic angiography. *Veterinary Radiology & Ultrasound* 59 (6): 677–686. <https://doi.org/10.1111/vru.12679>.
- Van den Ingh, T.S.G.A.M., J. Rothuizen, and H.P. Meyer. 1995. Circulatory disorders of the liver in dogs and cats. *Veterinary Quarterly* 17 (2): 70–76. <https://doi.org/10.1080/01652176.1995.9694536>.
- Vauthey, J.N., R.J. Tomczak, T. Helmberger, P. Gertsch, C. Forsmark, J. Caridi, A. Reed, M.R. Langham, G.Y. Lauwers, P. Goffette, and L. Lerut. 1997. The arterioportal fistula syndrome: *linicopathologic features, diagnosis, and therapy*. *Gastroenterology* 113 (4): 1390–1401. <https://doi.org/10.1111/jsap.13315>.
- Von Stade, L.E., S.B. Shropshire, S. Rao, D. Twedt, and A.J. Marolf. 2021. Prevalence of portal vein thrombosis detected by computed tomography angiography in dogs. *Journal of Small Animal Practice* 62 (7): 562–569. <https://doi.org/10.1111/jsap.13315>.
- Zwingenberger, A.L., R.C. McLearn, and C. Weisse. 2005. Diagnosis of arterioportal fistulae in four dogs using computed tomographic angiography. *Veterinary Radiology & Ultrasound* 46 (6): 472–477. <https://doi.org/10.1111/j.1740-8261.2005.00086.x>.

Publisher's Note

Springer Nature remains neutral with regard to jurisdictional claims in published maps and institutional affiliations.

Ready to submit your research? Choose BMC and benefit from:

- fast, convenient online submission
- thorough peer review by experienced researchers in your field
- rapid publication on acceptance
- support for research data, including large and complex data types
- gold Open Access which fosters wider collaboration and increased citations
- maximum visibility for your research: over 100M website views per year

At BMC, research is always in progress.

Learn more biomedcentral.com/submissions

